Eur. Phys. J. D **32**, 161–166 (2005)
DOI: 10.1140/epjd/e2005-00017-9

THE EUROPEAN PHYSICAL JOURNAL D

Long-term stability of continuous-wave emission from an ion-cavity system

M. Keller[1,a], B. Lange[1], K. Hayasaka[2], W. Lange[1,3,b], and H. Walther[1]

[1] Max-Planck-Institut für Quantenoptik, Hans-Kopfermann-Str. 1, 85748 Garching, Germany
[2] National Institute of Information and Communications Technology, 588-2 Iwaoka, Nishi-ku, Kobe 651-2492, Japan
[3] University of Sussex, Brighton, BN1 9QH, UK

Received 9 September 2004 / Received in final form 23 December 2004
Published online 9 February 2005 –

Abstract. Combining the technologies of ion-trapping and cavity quantum-electrodynamics, we have achieved uninterrupted coupling of a single ion to a mode of an optical resonator up to a time-scale of 10^3 seconds. The interaction of ion and field was implemented as a cavity-assisted Raman-transition from the ground state to an excited metastable state. The coupling was probed by detecting the photons emitted from the resonator upon excitation of the cavity mode. We have optimized the system parameters to obtain a high emission-rate. The experiment provides a basis for the controlled generation of single-photon pulses and other cavity quantum-electrodynamics effects relying on the continuous interaction of a single particle with a quantized field.

PACS. 32.80.Pj Optical cooling of atoms; trapping – 42.50.Ct Quantum description of interaction of light and matter; related experiments

1 Introduction

Experiments in the field of cavity quantum-electrodynamics (CQED) [1] explore the dynamics of single atoms coupled to a single mode of the electromagnetic field. When the strength of the coupling exceeds the rate of spontaneous emission and damping of the cavity field, the coherent exchange of excitation between atom and photon is the dominating process. CQED has thus become one of the most important tools in the investigation of quantum phenomena of the atom-field interaction. Strong coupling in the optical regime has been achieved using cavities with small mode-volume and mirrors with ultra-low losses [2]. Recently, an application of strongly coupled atoms and photons has emerged in the field of quantum computation. Here, the objective is to use the evolution of a quantum system to perform computation more efficiently than is possible in classical systems. The properties of CQED systems make them prime candidates for controlled quantum information processing [3]. In recent major advances towards this goal, field states with a single photon have been produced from a single atom, in the optical domain [4,5] and at microwave frequencies [6].

In order to use optical CQED systems for controlled quantum operations, one of the most important tasks is to permanently localize atoms in the cavity within a wavelength of the radiation (Lamb-Dicke localization). The reason is that due to the standing wave-structure in the axial direction, the cavity field varies on a scale set by the wavelength. Therefore, controlled coupling is only possible, if the atom's position is controlled with the same precision. In early optical CQED-experiments with atoms, the particles were traversing the cavity on random trajectories, resulting in random coupling with the field. A definite atomic position could only be obtained post-selectively by detecting the photons leaking from the cavity [7,8]. The position control was improved by using off-resonant dipole-trapping of the atoms [9]. However, fluctuations in g as large as 66% are still present [10]. By contrast, in recent experiments the Lamb-Dicke criterion was met for a calcium ion coupled to a cavity by exploiting the strong localization provided in a radio-frequency ion-trap [11,12]. A well-defined atom-cavity coupling is essential for controlling the system dynamics deterministically.

The present paper describes our recent experimental accomplishments in coupling a single calcium ion to an infrared cavity mode over extended times. The excitation scheme employed in the present paper uses continuous-wave pumping and repumping of the ion. This is in contrast to a recent experiment, in which we have produced single photons by pulsed excitation of the ion [13,14]. Through continuous pumping, we achieve a photon flux from the cavity output which is 100 times higher than in

[a] e-mail: Keller@mpq.mpg.de
[b] e-mail: W.Lange@sussex.ac.uk

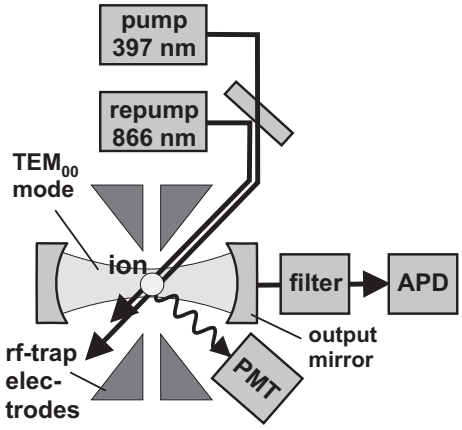

Fig. 1. Experimental set-up for coupling a single ion to a cavity mode. Pump- and repump-lasers are continuously injected from the side of the cavity. The cavity output is detected with an avalanche photodiode (APD), the UV-fluorescence of the ion with a photomultiplier (PMT). Not shown are the reference laser for locking the cavity frequency and an additional UV-beam for probing the micromotion component orthogonal to the pump-beam.

the pulsed case. The scheme described in the present paper is therefore better suited to probe the stability of the system at intermediate time scales down to 10 seconds.

After introducing the set-up of our system in Section 2, we discuss the cavity-assisted Raman coupling as the process linking the cavity field and an ion with a Λ-type level scheme (Sect. 3). In Section 4, we investigate the long-term stability of the ion-field coupling. We conclude with a discussion of future applications of the coherent manipulation of the ion-photon dynamics (Sect. 5).

2 Experimental set-up

In the experiment presented, photons are continuously generated with a single $^{40}Ca^{+}$-ion coupled to a single mode of an optical cavity. Prior to the measurement, an ion is loaded in the trap by photo-ionization of an atomic calcium-beam. Loading inside the cavity would expose the mirrors to coating with calcium, leading to mirror losses and unstable trapping conditions. Therefore, we use a linear trap and load it in a region spatially separated from the cavity zone [15]. Radial confinement is provided by applying a radio-frequency (rf) voltage of 400 V at 12.7 MHz to four electrodes in a quadrupole mass-filter arrangement (shown in cross-section in Fig. 1), resulting in a harmonic pseudopotential with an ion oscillation frequency of 1.3 MHz. In the axial direction, the position of the ions is controlled with five pairs of dc-electrodes, located in the vertical gap between the rf-electrodes. By applying a voltage of 20 V, harmonic axial confinement at a frequency of 300 kHz is achieved. After loading the trap, the ions are shuttled to the cavity region by sequentially ramping the voltage at the dc-electrodes [15].

Residual electric stray-fields may be present in the trap, shifting the equilibrium position of the ion off the nodal line of the rf-field. Since this would lead to an oscillation of the ion, driven by the trapping field (micromotion), radial dc-fields must be compensated with correctional dc-voltages applied to the rf-electrodes. The optimal ion position is determined by minimizing the modulation of the ultraviolet (UV) fluorescence intensity (see below) due to the micromotion-induced Doppler-effect. Two non-collinear probe beams are used for compensating both transverse directions.

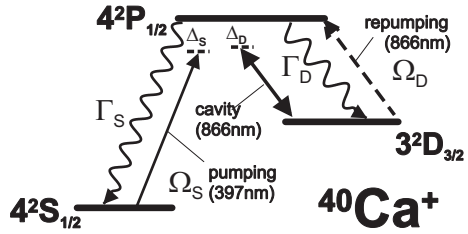

Fig. 2. Level scheme of $^{40}Ca^{+}$, indicating the wavelengths and decay channels of the transitions relevant for cavity-QED. Cavity and pump-laser are represented by solid lines. The dashed transition is used for repumping.

Figure 2 shows the levels of singly ionized calcium relevant for our photon generation scheme. The $S_{1/2}$ ground state, the $P_{1/2}$ exited state and the $D_{3/2}$ metastable state with a 1 second lifetime form a Λ-system. The optical cavity is close to resonance with the $D_{3/2}\rightarrow P_{1/2}$-transition at a wavelength of 866 nm. By coupling the cavity to an infrared (IR) transition, we take advantage of the small absorption and scattering losses of the dielectric coating in this wavelength range. Minimizing optical losses is essential for observing CQED effects, which depend on a small damping of the cavity field.

The ion is driven by a pump-beam at a wavelength of 397 nm, obtained from a frequency-doubled Ti:sapphire laser and injected from the side of the cavity, as shown in Figure 1. The laser has a linewidth below 500 kHz. Its frequency is referenced to a diode laser locked to the D_2-line of atomic cesium by means of a scanning Fabry-Perot resonator, eliminating any frequency drift of the laser [16]. We excite the resonator-field by means of a cavity-assisted Raman-transition between $S_{1/2}$ and $D_{3/2}$, which is off resonance with the $P_{1/2}$-level, in order to suppress spontaneous Raman-scattering. The detuning of pump-beam and cavity from the upper $P_{1/2}$-level is typically 10 to 30 MHz.

The cavity is formed by two mirrors with radius of curvature 1 cm, fitting in the horizontal gap between the electrodes (Fig. 1). The cavity axis is oriented perpendicular to the trap axis and the length of the cavity is 8 mm. For optimum coupling, the cavity is tuned to Raman resonance with the pump-pulse. The cavity must have a frequency stability better than the linewidth of the Raman-resonance to maintain stable operating conditions. Therefore, the cavity frequency is locked to a reference diode laser at 894 nm, optically locked to a confocal cavity mounted on an invar-spacer. The 28 nm detuning of the reference laser from the $D_{3/2}\rightarrow P_{1/2}$-transition, guarantees a negligible perturbation of the ion. With an acousto-optic modulator, the frequency of the reference laser is shifted

to resonance with a suitable high-order transverse mode of the cavity. The stabilisation signal is obtained by measuring the cavity transmission of the reference laser with a photodiode and a lock-in amplifier and by feeding back the error signal to a piezo actuator controlling the cavity-length. In this way, we reach a short-term frequency stability of better than 50 kHz with respect to the reference laser, limited entirely by electronic noise. To prevent long-term drift of the cavity frequency, the reference laser is kept resonant with the D_1-line of atomic Cs at 894 nm by feeding back on the length of the optical locking cavity.

In addition to the pump-laser, a diode laser at 866 nm is applied to repump on the $D_{3/2} \rightarrow P_{1/2}$-transition. In this way, population trapping in the long-lived $D_{3/2}$-state is avoided and continuous-wave emission from the cavity is maintained. The repump-laser is optically locked to the same confocal cavity used for stabilizing the reference laser, resulting in a linewidth of 200 kHz. Since the length of the confocal cavity is locked to the D_1-line of Cs, frequency drift of the repumping laser is avoided. The repump-laser is tuned slightly to the blue of the atomic transition, far detuned from Raman-resonance with either the pump-laser or the cavity-mode. Therefore, creation of a dark state with the repump-laser is prevented.

Apart from its role in driving the Raman transition, the red-detuned pump-laser is employed to Doppler-cool the ion. Therefore, the angle under which the pump-beam is injected is chosen to provide cooling along all three principal axes of the trap. A fraction of the UV fluorescent light emitted in the process of Doppler-cooling is collected with a lens mounted on the side of the cavity and detected by focusing it on a photomultiplier tube. The signal is used to establish the presence of the ion in the cavity and to diagnose the internal and motional state of the ion in the trap, for example the micromotion mentioned above.

To detect the emission of the ion into the cavity-mode, the signal transmitted through the output mirror is focussed on an avalanche photodiode (APD) with a detection efficiency of about 30% at 866 nm. Care must be taken not to expose this detector to radiation from the reference laser beam at 894 nm, which has an intensity as large as 1 nW on resonance, required to obtain a suitable locking signal from the photodiode. This is 10^6 times more intense than the cavity emission at 866 nm for an ion optimally coupled to the cavity. We separate the two signals by using a set of four spectral filters, obtaining an attenuation of the reference laser of 10^{-11} in the 866 nm channel. By additional spatial filtering, stray light is largely suppressed. With this combination of filters, we reduce the intensity of background light to below the dark-count rate of the APD ($\geqslant$50 Hz). A fraction of 4.6% of the photons emitted from the cavity is detected. Apart from the detection efficiency of the APD, propagation losses, in particular in the filter assembly, contribute to the loss of photons.

3 Coupling of ion and cavity-mode

The two long-lived states of the ion, the ground state $S_{1/2}$ and the metastable state $D_{3/2}$ are coupled to the cavity through an off-resonant Raman transition. As described above, it is driven by the 397 nm pump-laser, with the cavity field acting as the Stokes component. Both cavity and pump-laser are detuned from the excited $P_{1/2}$-level by the same amount ($\Delta_S = \Delta_D = \Delta$), so that they are at Raman resonance with the ion. The AC-Stark shift of the Raman resonance due to the pump lasers is negligible compared to the width of the Raman resonance and can be absorbed in the definition of Δ_S. The effective coupling between atom and field on this transition is then

$$g_{\text{eff}} = \frac{g\Omega_S}{2\Delta}, \tag{1}$$

where Ω_S is the Rabi-frequency of the pump-beam driving the UV-transition and g the ion-field coupling. The quantity g_{eff} is the rate at which ion and cavity-field coherently exchange their excitation and therefore is a crucial parameter for the dynamics of the system. It must be compared with the decay rate κ of the cavity field amplitude due to the finite transmissivity of the mirrors as well as scattering and absorption losses. Typical values, realized in the experiment with a cavity of 8 mm length, are $(\Omega_S, g, \Delta, \kappa)/2\pi = (9, 0.9, 20, 1.2)$ MHz, so that the effective coupling is on the order of 0.2 MHz.

The above parameters imply $g_{\text{eff}} < \kappa$, so that the experiment is operated in the bad cavity regime of CQED. Under these conditions, a cavity photon generated in the Raman process has only a small probability to be reabsorbed by the ion. Instead, the most likely event is the leakage of the photon through the output mirror. In our set-up, this is a mirror with a transmissivity of 600 ppm, much larger than that of the second mirror at 5 ppm.

The finite transmissivity of the output mirror and the resulting emission from the cavity provides us with the opportunity to observe the coupling between ion and cavity through the rate at which photons emerge from the cavity output. Assuming that the repumping laser is intense enough to efficiently return population from $D_{3/2}$ to the ground state, and for pump-intensity $|\Omega_S|^2$ well below saturation, the rate of cavity-emission at Raman-resonance, derived from the effective Raman coupling of equation (1), is proportional to the rate of cavity-mediated atomic damping

$$R_{\text{cav}} \sim \frac{g_{\text{eff}}^2}{\kappa} = \frac{g^2\Omega_S^2}{4\kappa\Delta^2}. \tag{2}$$

A measurement of this rate is presented in Figure 3a. We have probed the Raman-resonance of the cavity-mode and the pump-laser by scanning the detuning Δ_S of the laser for four different values of the cavity detuning Δ_D. The peaks in the cavity emission indicate Raman-resonance. The decreasing amplitude of cavity emission at Raman-resonance for larger detunings Δ_D, predicted by equation (2), is clearly confirmed by comparing the four traces in Figure 3a. In the figure, Lorentzian curves have been fitted to the Raman resonance line. The linewidth was used as an adjustable parameter to accommodate deviations from the idealized model used in reference [14].

Apart from the detunings, important parameters for the emission characteristics are the intensities of the

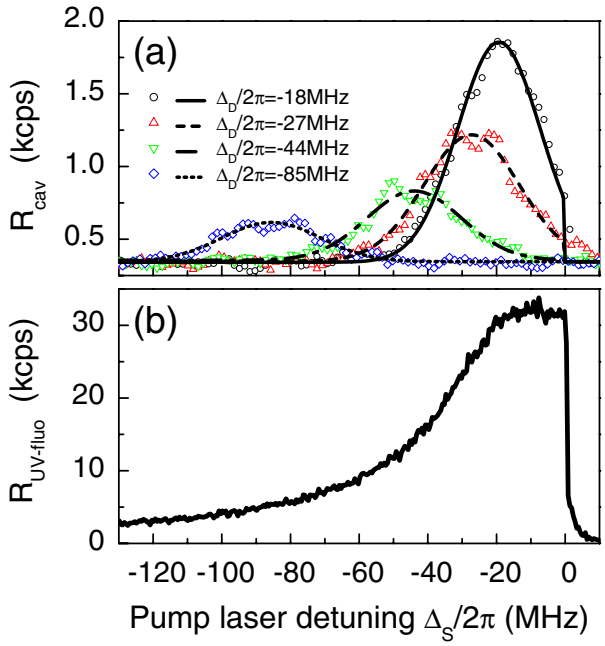

Fig. 3. (a) Cavity output rate as a function of the detuning of the pump-laser. The different traces correspond to different detunings Δ_D of the cavity, resulting in a corresponding shift of the Raman resonance: $\Delta_D/2\pi = (-18, -27, -44, -85)$ MHz. (b) UV-fluorescence emitted to the side of the cavity as a function of the detuning of the pump-laser.

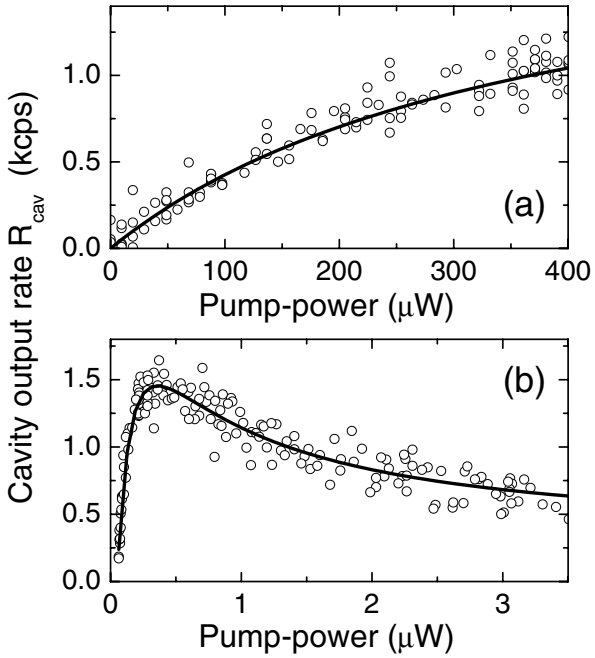

Fig. 4. Cavity output rate as a function of (a) the power of the UV pump-beam; (b) the power of the IR repump-beam. The solid line is a theoretical fit based on a three-level model of the calcium-ion [17], using the coupling of the UV- and IR-beams to the ion as well as the detection efficiency as free parameters.

pump- and repump-laser. Their influence on the rate of cavity emission is presented in Figure 4. According to Figure 4a, the cavity output rate is increasing monotonically as a function of the UV pump-power and saturating at large intensities. By contrast, in a scan of the IR repump-power in Figure 4b, the cavity emission shows a pronounced maximum. At low IR-intensity, the emission increases due to more efficient repumping. The drop in the output rate at larger repump-intensity is a consequence of the AC-Stark shift induced by the repump-laser. It tunes the cavity and the pump-laser out of Raman-resonance, leading to decreased photon production and hence decreased cavity emission.

A process competing with the generation of a cavity photon in the Raman process is the off-resonant excitation of the $P_{1/2}$-level, followed by spontaneous emission of a fluorescence photon either on the ultraviolet transition leading to the ground state or on the infrared transition to the metastable state. In the limit of large detuning of the Raman resonance ($\Delta \gg \Gamma_S \gg \Gamma_D$) and a repumping beam close to resonance, the respective rates are

$$\Gamma_{\text{eff}}^{S} \approx \Gamma_S \frac{\Omega_S^2}{4\Delta^2}, \tag{3}$$

$$\Gamma_{\text{eff}}^{D} \approx \Gamma_D \frac{\Omega_S^2}{4\Delta^2}. \tag{4}$$

In the experiment, the spontaneous emission rates are $\Gamma_S/2\pi = 22.3$ MHz and $\Gamma_D/2\pi = 1.7$ MHz. The ultraviolet transition is the dominant decay channel. In particular for small Δ, several UV photons may be emitted before a cavity photon is generated. The dependence of the ultraviolet fluorescence intensity on the pump-detuning is shown in Figure 3b. Taking into account the overall detection efficiency below 1% for UV-photons, a comparison of panels a and b in Figure 3 confirms the strong contribution of UV-scattering, which at resonance is 50 times more likely than cavity emission. It should be noted that, while the presence of UV-scattering reduces the rate of photon emission from the cavity, the scaling of the cavity output rate with the system parameters is still accurately described by equation (2).

4 Long-term stability of the ion-field coupling

One of the most important advantages of CQED with a single trapped ion is that the particle remains localized for many hours. An ion which is stationary with respect to the field distribution experiences continuous coupling to the cavity field at constant g. This is essential for schemes of quantum information processing, where the controlled and reversible interaction of ions and photons can be achieved only if the coupling is well-defined for the entire duration of the computation. A related application is the deterministic generation of single-photon pulses *on demand*. Since there is no a priori knowledge of the required emission time, a trigger signal can be processed successfully only if a deterministically coupled ion is present in the cavity at all times.

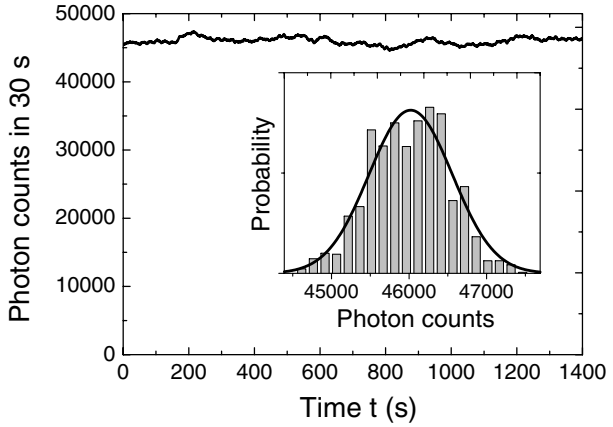

Fig. 5. Cavity-output counts monitored over 1400 seconds. The data are displayed using a running average over $\tau = 30$ s. The inset shows the statistical distribution of photon counts in this measurement for a bin-width of 150 counts.

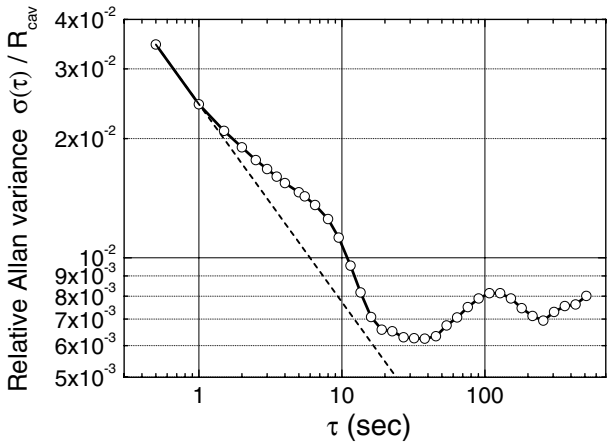

Fig. 6. Relative overlapping Allan standard deviation of the cavity output rate $R_{\rm cav}$ detected with the avalanche photodiode at the cavity output. An average of 770 counts is registered in each 500 ms interval. The dashed line corresponds to the shot-noise associated with the detected photon counts.

In order to assess the stability of ion-field coupling at large time scales, we have monitored the cavity output for an extended time (30 minutes), with a single $^{40}Ca^{+}$-ion optimally coupled to the TEM_{00}-mode of the cavity. Both the frequency of the cavity-mode and the frequency of the UV pump-beam were red-detuned with respect to $P_{1/2}$ by slightly less than the natural linewidth of the UV-transition ($\Delta_D = \Delta_S \lesssim \Gamma_S$), to establish Raman-resonance. The resulting time-series of photon counts, averaged over 30 s is plotted in Figure 5. It shows the stability of the cavity emission and thus the ion-cavity coupling on this time-scale.

The stability of the cavity output rate $R_{\rm cav}$ on different time scales may be quantified by means of the Allan variance [18]. With a photon count-rate of 1.5×10^3 s^{-1} and a total measurement time of 30 minutes, we have statistically evaluated our data using integration windows from 500 ms to 500 s. The relative overlapping Allan standard deviation $\sigma(\tau)/R_{\rm cav}$ in this range is shown in Figure 6.

Below $\tau = 20$ s, $\sigma(\tau)$ decreases roughly with a $\tau^{-1/2}$ dependence. This corresponds to a white-noise spectrum at frequencies above 0.05 Hz, which is expected for the shot noise associated with our photon count rate. In Figure 6 excess noise appears at timescales around 8 s, leading to a deviation from the expected $\tau^{-1/2}$-behaviour, and as an additional peak in the standard deviation around $\tau \approx 100$ s. Both contributions we tentatively attribute to technical sources. At the same time there is a gradual increase of the Allan variance, indicating a slow drift of the cavity output intensity. Note that due to the relatively high photon count rates in the continuously pumped system, the shot noise affects only time scales below 20 s. This is in contrast to operating the system as a single-photon source, which has a much lower countrate and hence larger shot noise contributions [14].

The lower limit of the relative Allan variance, reached at $\tau = 30$ s corresponds to $\sigma_{\rm min}/R_{\rm cav} \approx 6 \times 10^{-3}$. Assuming that the fluctuations in $R_{\rm cav}$ are caused entirely by fluctuations in the coupling g, which appears quadratically in equation (2), we obtain an upper limit for the minimum relative standard deviation of g, averaged over 30 s:

$$\frac{\sigma^g_{\rm min}}{g} \leqslant \frac{1}{2}\frac{\sigma_{\rm min}}{R_{\rm cav}} = 3 \times 10^{-3}. \qquad (5)$$

However, the actual size of the fluctuations of g is expected to be even smaller, since other sources of noise increase the measured Allan variance of the output intensity. Fluctuations of the intensity of the pump-laser are a major source of noise in $R_{\rm cav}$, which in the limit of small pump-intensities is proportional to $|\Omega_S|^2$, according to equation (2). Since the pump-intensity is not stabilized in the experiment, it is subject to a slow drift consistent with the increase of $\sigma(\tau)$ for $\tau > 30$ s apparent from Figure 6. Frequency fluctuations are not expected to contribute to the noise significantly, since, as explained in Section 2, the short-term and the long-term stability of pump-laser and cavity are well below the width of the Raman resonances presented in Figure 3.

The small fluctuations of g averaged over tens of seconds confirm the degree of control we have over the ion-field coupling at those time scales. For much smaller times, no estimates of the stability of g can be extracted from the cavity-output signal, due to the limited photon count-rates available, leading to large shot-noise. The coupling constant g is subject to fluctuations mainly due to the position uncertainty of the particle under study. This is, in fact, a significant difficulty in single-*atom* CQED. With ions, much better localization and hence more stable coupling can be obtained [11]. The long-term and the short-term stability of the coupling g between ion and cavity is therefore expected to be better than the upper limit quoted in equation (5).

5 Conclusions

In this paper, we have investigated the Raman-coupling of a single ion to a single mode of a high finesse cavity. It provides an interface between atomic quantum states and photons at the single quantum level. The dynamical process underlying the generation of an infrared cavity-photon from an atom in the atomic ground state is the cavity-enhanced, off-resonant Raman-scattering of an ultraviolet pump-photon, provided the cavity is tuned to the Stokes frequency.

In order to find the optimum operating parameters, we have maximized the cavity output as a function of the relative detuning of pump and cavity and the intensities of pump- and repump-laser. An essential advantage of using an ion as a medium for CQED is the long storage-time provided by the trap, together with a strong localization. We have exploited the deterministic coupling of ion and field to emit a continuous stream of photons from the cavity-output for up to 30 minutes. We have analyzed the fluctuations of the cavity emission rate on time-scales ranging from 500 ms to 500 s, with the lowest standard deviation measured for an averaging time of 30 s. The result provides an upper limit of 3×10^{-3} relative fluctuations of g on that time-scale. The actual stability of the coupling is expected to be even better, since other factors contribute to the observed cavity-output fluctuations.

The duration of stable coupling between ion and field is three orders of magnitude larger than previous experiments with atoms. Thus, our set-up provides the basis for truly deterministic CQED with single particles. An example is the controlled generation of single-photon pulses [4,5,13,19], which is required in applications such as secure quantum communication protocols [20] and linear optics quantum computation [21]. A crucial advantage of single-atom CQED systems is that the interaction via an off-resonant Raman-transition is fully coherent and therefore single-photon emission is in principle reversible. Our system may therefore serve as a building block of a quantum network [22], which accepts and emits single photons on demand, converting quantum information between atomic and photonic degrees of freedom. In this way, the advantages of photons for long-distance transfer and ions for local processing and storage of quantum information may be ideally combined.

References

1. *Cavity quantum electrodynamics*, edited by P.R. Berman (Academic Press, San Diego, 1994)
2. H.J. Kimble, Phys. Scripta **T76**, 127 (1998)
3. C. Monroe, Nature **416**, 238 (2002)
4. J. McKeever, A. Boca, A.D. Boozer, R. Miller, J.R. Buck, A. Kuzmich, H.J. Kimble, Science **303**, 1992 (2004)
5. A. Kuhn, M. Hennrich, G. Rempe, Phys. Rev. Lett. **89**, 067901 (2002)
6. S. Brattke, B.T.H. Varcoe, H. Walther, Phys. Rev. Lett. **86**, 3534 (2001)
7. C.J. Hood, T.W. Lynn, A.C. Doherty, A.S. Parkins, H.J. Kimble, Science **287**, 1447 (2000)
8. P.W.H. Pinkse, T. Fischer, P. Maunz, G. Rempe, Nature **404**, 365 (2000)
9. J. McKeever, J.R. Buck, A.D. Boozer, A. Kuzmich, H.C. Nagerl, D.M. Stamper-Kurn, H.J. Kimble, Phys. Rev. Lett. **90**, 133602 (2003)
10. L.M. Duan, A. Kuzmich, H.J. Kimble, Phys. Rev. A **67**, 032305 (2003)
11. G.R. Guthöhrlein, M. Keller, K. Hayasaka, W. Lange, H. Walther, Nature **414**, 49 (2001)
12. A.B. Mundt, A. Kreuter, C. Becher, D. Leibfried, J. Eschner, F. Schmidt-Kaler, R. Blatt, Phys. Rev. Lett. **89**, 103001 (2002)
13. M. Keller, B. Lange, K. Hayasaka, W. Lange, H. Walther, Nature **431**, 1075 (2004)
14. M. Keller, B. Lange, K. Hayasaka, W. Lange, H. Walther, Appl. Phys. B (submitted)
15. M. Keller, B. Lange, K. Hayasaka, W. Lange, H. Walther, Appl. Phys. B **76**, 125 (2003)
16. W.Z. Zhao, J.E. Simsarian, L.A. Orozco, G.D. Sprouse, Rev. Sci. Instrum. **69**, 3737 (1998)
17. G. Janik, W. Nagourney, H. Dehmelt, J. Opt. Soc. Am. B **2**, 1251 (1985)
18. D.W. Allan, Proc. IEEE **54**, 221 (1966)
19. C.K. Law, H.J. Kimble, J. Mod. Opt. **44**, 2067 (1997)
20. C.H. Bennett, G. Brassard, In *Proc. IEEE Int. Conf. Comp. Syst. Sig. Process.*, Bangalore, India, pp. 175–179, New York (1984)
21. E. Knill, R. Laflamme, G.J. Milburn, Nature **409**, 46 (2001)
22. J.I. Cirac, P. Zoller, H.J. Kimble, H. Mabuchi, Phys. Rev. Lett. **78**, 3221 (1997)